J. Synchrotron Rad. (1998). **5**, 880–882

Detailed simulation of the response function of an Si(Li) detector

Shunji Goto

Japan Synchrotron Radiation Research Institute, SPring-8, Kamigori 678-12, Japan. E-mail: sgoto@spring8.or.jp

(*Received 4 August 1997; accepted 1 December 1997*)

The response function of an Si(Li) detector was calculated by using a Monte Carlo method for photon energies below 10 keV. In the simulation, electron elastic-scattering cross sections calculated using the partial-wave expansion method were used instead of the Born approximation to simulate the electron scattering more accurately. The carrier collection probability near the gold–silicon interface was derived by solving the carrier continuity equation with drift, diffusion and surface recombination by a finite recombination velocity. For two detectors, good agreement was found for low-energy tailing between measured and simulated response functions. The integrated detection efficiency is almost identical with the transmittance in the front gold electrode showing a maximum difference of 2% at the Au M_4-absorption edge.

Keywords: Si(Li) detectors; response functions; Monte Carlo simulations.

1. Introduction

The detection efficiency and response function of an Si(Li) detector must be determined when it is used in high-precision measurements. The detection efficiency of the Si(Li) detector decreases due to X-ray absorption in the beryllium window, gold electrode and silicon dead layer for low-energy X-rays. Distortion of spectra due to escape peak and low-energy tailing (tail and flat continuum) is also observed, especially below 5 keV (Krumrey *et al.*, 1989; Scholze & Ulm, 1994). The shape of the response function varies markedly depending on the photon energy. A Monte Carlo simulation code was developed for photon energies below 10 keV (Goto, 1993). Although it provides the physical reason for the tailing for energies below 10 keV qualitatively, there is a difference in the amount of flat continuum near the zero channel. According to the simulation, the gold electrode provides the main contribution to the flat continuum near the zero channel. In this code, screened Rutherford cross sections were used to calculate the electron scattering angle and mean free path. However, this is not valid for low-energy electrons and high-Z elements. Therefore, more accurate cross sections calculated using the partial-wave expansion methods have been tested in the present simulation.

In this report, it is shown that a better treatment of the electron scattering processes improves the simulation. The integrated detection efficiency is also discussed, based on the simulation.

2. Calculation of the response function

Nine possible processes near the detector surface concerning the absorption of incident photons, emissions of photoelectrons, Auger electrons and Si $K\alpha$ are considered in the simulation, as shown in Fig. 1. The Si $K\alpha$ X-rays may be absorbed in the detector again and generate the photoelectrons (the Auger process is neglected in this case), or escape from the surface, which gives the escape peak. The ten most intense *MNN* Auger transitions for the *M*-shell absorption of gold are considered, in contrast with the three most intense transitions in the previous simulation (Goto, 1993). Energy losses of electrons and the creation of charge carriers and charge losses near the detector surface due to surface recombination are considered as successive processes.

The photoelectrons and Auger electrons are scattered by atoms and lose their energies, creating charge carriers along their trajectories in the sensitive silicon region. In the previous code, the screened Rutherford (Sc. R) cross sections based on the Born approximation were used to calculate the electron scattering angle and mean free path. However, this is not valid for low-energy electrons below 20 keV and high-Z elements such as gold (Ichimura & Shimizu, 1981). A Monte Carlo calculation using the Sc. R cross sections shows a smaller electron range than experimental values (Kotera *et al.*, 1981). Therefore, more accurate cross sections were calculated using the partial-wave expansion method (PWEM) (Ichimura & Shimizu, 1981; Jablonski *et al.*, 1989). The Thomas–Fermi–Dirac potentials were used for silicon and gold atoms. The continuous slowing-down approximation was used for the electron energy loss.

To obtain the carrier collection probability as a function of the position where carriers are generated, a simple model was introduced which takes into account drift, diffusion and reflections due to a finite surface recombination velocity (Goto, 1993). More detailed treatment of this model is shown here.

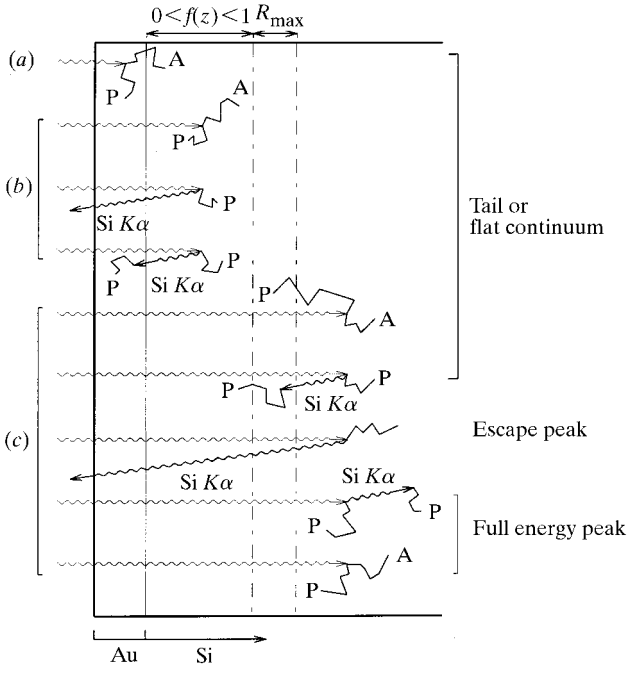

Figure 1
Nine possible processes near the detector surface concerning absorption of the incident photons, emissions of photoelectrons (P), Auger electrons (A), and Si $K\alpha$. R_{max} is the maximum electron range, $f(z)$ is the carrier collection function.

The carrier continuity equation is given by

$$\frac{\partial n(z,t)}{\partial t} = -v\frac{\partial n(z,t)}{\partial z} + D\frac{\partial^2 n(z,t)}{\partial z^2}, \tag{1}$$

with boundary condition and initial condition

$$-D\frac{\partial n(0,t)}{\partial z} + vn(0,t) = -sn(0,t), \tag{2}$$

$$n(z,0) = \delta(z - z_0), \tag{3}$$

where n is the carrier (electron) density, z is the carrier generation position measured from the gold–silicon interface, t is the time after the carrier generation, s is the surface (interface) recombination velocity, v is the drift velocity, D is the effective diffusion coefficient and z_0 is the initial carrier generation position. The solution of the carrier continuity equation is given by

$$\begin{aligned} n(z,t) = (4\pi Dt)^{-1/2}\{&\exp[-(z - z_0 - vt)^2/4Dt] \\ &+ \exp[-(z + z_0 - vt)^2/4Dt - vz_0/D]\} \\ &- [(v + 2s)/2D]\exp[(s + v)(z + z_0 + st)/D - vz_0/D] \\ &\times \operatorname{erfc}\{[z + z_0 + (v + 2s)t]/2(Dt)^{1/2}\}, \end{aligned} \tag{4}$$

where $\operatorname{erfc}(x)$ is the complementary error function:

$$\operatorname{erfc}(x) \equiv 1 - (2/\pi^{1/2})\int_0^x \exp(-t^2)\,\mathrm{d}t. \tag{5}$$

The carrier collection probability is calculated by integrating (4) and by taking the limit

$$\begin{aligned} f(z_0) &= \lim_{t\to\infty}\int_0^\infty n(z,t)\,\mathrm{d}z = 1 - [s/(s + v)]\exp(-vz_0/D) \\ &= 1 - [1 - v/(s + v)]\exp(-vz_0/D) \\ &= 1 - (1 - R)\exp(-vz_0/D). \end{aligned} \tag{6}$$

where R is the carrier reflectivity at the gold–silicon interface. This equation agrees with a previous one (Goto, 1993). Infinite surface recombination velocity gives no carrier collection probability at the gold–silicon interface. For large z, the carrier collection probability becomes unity. For the case of finite recombination velocity, the probability decreases towards the interface but it does not become zero. The value D/v is estimated to be about 0.1 μm (Goto, 1993). The values s, v and D characterize the incomplete carrier collection region (dead layer).

Fig. 2 schematically shows trajectories of photoelectrons and Auger electrons, including emission direction after absorption of photon, elastic scattering of the electrons, and energy loss between elastic scattering. For each photon, the fraction of carriers collected by the detector is calculated by summing the product of energy loss in the free path of elastic scattering, $\Delta E(z)$, and the carrier collection probability, $f(z)$, along the electron trajectories. The collected carrier number is given by

$$N = \sum_j \sum_i [\Delta E_i(z)/\varepsilon]\int_{z_{i-1}}^{z_i} f(z)\,\mathrm{d}z \Big/ (z_i - z_{i-1}), \tag{7}$$

where ε is the mean energy to create an electron–hole pair, i is the step of electron scattering and j are the electron energy-loss processes of photoelectrons and Auger electrons. By calculating the carrier number for each photon, the response function can be obtained.

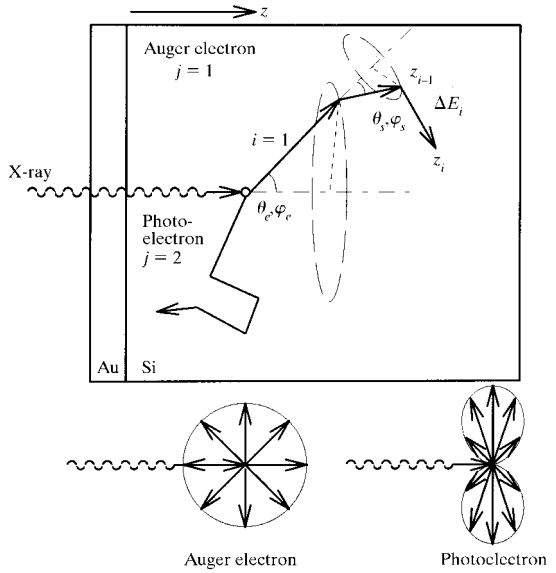

Figure 2
Trajectories of Auger electrons and photoelectrons, including emission direction after absorption of photon, elastic scattering of the electrons, and energy loss between elastic scattering.

3. Results

Fig. 3 shows calculated and measured response functions for 4 and 6 keV photons. Details of the measurements are given by Scholze & Ulm (1994) for Fig. 3(*a*) and Goto (1993) for Fig. 3(*b*). Besides the standard deviation of the photopeak width, the response

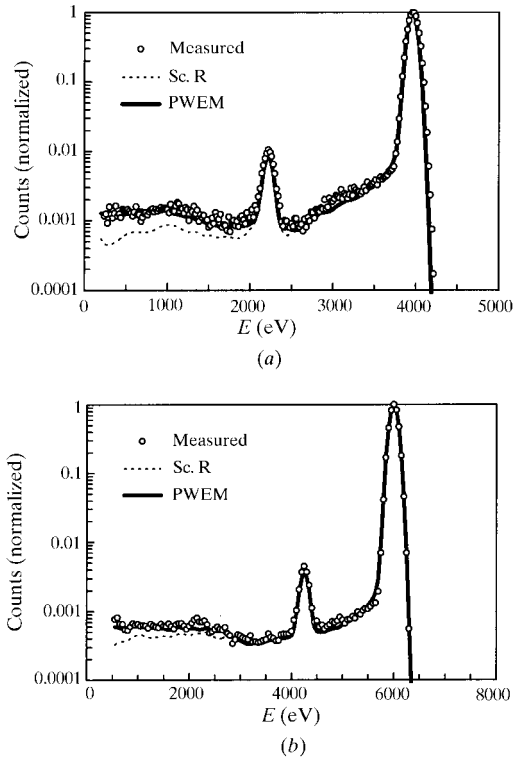

Figure 3
Measured and calculated response functions for two detectors. (*a*) For 4 keV photons; 37 nm-thick gold electrode, D/v = 0.1 μm and $R = v/(s+v)$ = 0.6 are assumed. (*b*) For 6 keV photons; 20 nm-thick gold electrode, D/v = 0.09 μm and R = 0.45 are assumed.

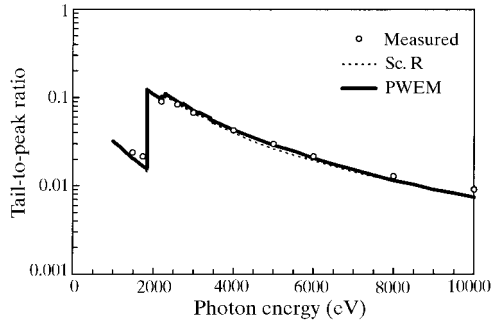

Figure 4
Tail-to-peak ratio for the detector (Goto, 1993).

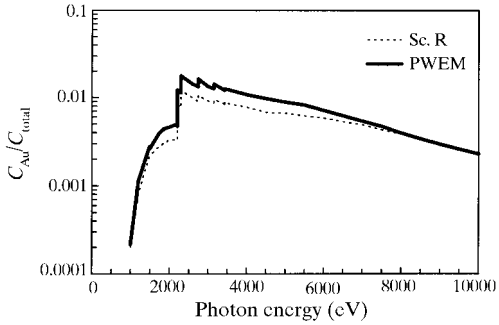

Figure 5
Contribution of the gold electrode to the response for the detector (Goto, 1993).

function can be basically simulated by only three parameters: gold electrode thickness, ratio of diffusion coefficient to drift velocity v/D, carrier reflectivity R. The fitting parameters in the simulation are v/D and R. The threshold of the tail beside the photopeak is explained by carrier reflection with reflectivity of 60% and 45%, respectively. Good agreement is clearly demonstrated using the cross sections by PWEM, especially at the flat continuum. Fig. 4 shows the tail-to-peak ratio as a function of the photon energy for the detector (Goto, 1993). From these results, the discrepancy between measurements and previous calculations (Sc. R) is explained to be due to the underestimation of the electron range.

Fig. 5 shows the ratio of the counted photons after absorption in the gold electrode (C_{Au}) to the total photons counted from photopeak to zero channel (C_{total}). There is a maximum contribution of C_{Au} of 2% at the Au M_4-absorption edge. This calculation predicts that the integrated detection efficiency (full energy peak and the low-energy tailing) is almost identical with the transmittance in the front gold electrode showing a maximum difference of 2% at the Au M_4-absorption edge. It describes well the experimental results of Scholze & Ulm (1994).

4. Conclusions

The response function of an Si(Li) detector was calculated by using the Monte Carlo method for photon energies below 10 keV. Good agreement between measured and simulated response functions was found by using PWEM instead of the Sc. R scattering model. The simulation results shows that the tail is mainly due to the imperfect carrier collection region and the threshold of the tail is due to carrier reflection at the gold–silicon interface, which depends on the detector. The results also show that the flat continuum is due to penetration of the electrons from the gold electrode to the silicon region and escape of the electrons from silicon to the gold electrode. The integrated detection efficiency is almost identical with the transmittance in the front gold electrode showing a maximum difference of 2%.

The author would like to thank Frank Scholze for his useful discussion about the response function and the detection efficiency, and for kindly offering the response-function data.

References

Goto, S. (1993). *Nucl. Instrum. Methods*, A**333**, 452–457.
Ichimura, S. & Shimizu, R. (1981). *Surf. Sci.* **112**, 386–408.
Jablonski, A., Gryko, J., Kraaer, J. & Tougaard, S. (1989). *Phys. Rev. B*, **39**, 61–71.
Kotera, M., Murata, K. & Nagami, K. (1981). *J. Appl. Phys.* **52**, 997–1003.
Krumrey, M., Tegeler, E. & Ulm, G. (1989). *Rev. Sci. Instrum.* **60**, 2287–2290.
Scholze, F. & Ulm, G. (1994). *Nucl. Instrum. Methods*, A**339**, 49–54.